Journal of Theoretical and Applied Information Technology
15th May 2021. Vol.99. No 9

ISSN: 1992-8645 www.jatit.org E-ISSN: 1817-3195

COMPARATIVE ANALYSIS OF UNIVERSAL METHODS NO REFERENCE QUALITY ASSESSMENT OF DIGITAL IMAGES

[1] ELMIRA ELDAROVA, [2] VALERY STAROVOITOV, [3] KAZIZAT ISKAKOV
[1,3]L.N. Gumilyov Eurasian National University, Nur-Sultan, Kazakhstan
[2]United Institute of Informatics Problems National Academy of Sciences of Belarus, Minsk, Belarus
E-mail: [1]doctorphd_eldarova@mail.ru, [2]valerystar@mail.ru, [3]kazizat@mail.ru

ABSTRACT

The main purpose of this article is to conduct a comparative study of two well-known no-reference image quality assessment algorithms BRISQUE and NIQE in order to analyze the relationship between subjective and quantitative assessments of image quality. As experimental data, we used images with artificially created distortions and mean expert assessments of their quality from the public databases TID2013, CISQ and LIVE. Image quality scores were calculated using the NIQE, BRISQUE functions and their average. The correlation coefficients of Pearson, Spearman and Kendall were analyzed between expert visual assessments and quantitative scores of the image quality, as well as between the values of three compared indicators. For the experiments, the Matlab system and values of its functions ***niqe*** and ***brisque*** normalized to the range [0, 1] were used. The computation time of ***niqe*** is slightly less. The investigated functions poorly estimate the contrast of images, but the additive Gaussian noise, Gaussian blur and loss in compression by the JPEG2000 algorithm are better. The BRISQUE measure shows slightly better results when evaluating images with additive Gaussian noise, while NIQE for blurred by Gaussian. The average of the normalized values of NIQE and BRISQUE is a good compromise. The results of this work may be of interest for the practical implementations of digital image analysis.

Keywords: *Image quality assessment, No-reference measure, Objective metrics, BRISQUE, NIQE*

1. INTRODUCTION

Recently, special attention has been paid to the development no reference quality assessment criteria which are not limited to a priori type of distortion. In practice, information about the type of distortion is not always available therefore the urgent task is to develop precisely universal algorithms that implement functions that can assess the image quality without a standard and without knowing the types of distortions. There are some such well-known algorithms: Distortion Identification-based Image Verity and INtegrity Evaluation (DIIVINE)[1]- which is a two-stage structure that includes distortion identification and distortion-specific quality assessment. It is built on NSS. In particular, a set of neighboring wavelet coefficients are modeled by a Gaussian scale mixture model. Also, steerable pyramid decomposition has been used to extract statistics from the distorted images. BLIINDS-II[2] obtains NSS features by discrete cosine transform coefficients modeling using generalized Gaussian distribution. The parameters of the generalized Gaussian distribution are applied as quality-aware features. Blind/referenceless image spatial quality evaluator (BRISQUE)[3] uses scene statistics of locally normalized luminance coefficients to train a support vector regressor (SVR) for perceptual quality prediction. Natural Image Quality Evaluator(NIQE) [4] measures the distance between the natural scene statistics (NSS) based features calculated from the pristine images to the features extracted from the input image. The features are modeled as multi-dimensional Gaussian distributions. Curvelet quality assessment (CurveletQA) [5]] extracted statistical features (the coordinates of the maxima of the log-histograms of the curvelet coefficients, the energy distributions of both orientation and scale in the curvelet domain) from the image's curvelet representation. Besides, image distortion and quality prediction stages have been trained using a support vector machine (SVM). Spatial–Spectral Entropy-based Quality (SSEQ) [6]] includes an image distortion and quality prediction engine. Moreover, it extracts a 12-dimensional local entropy feature vector. GRAD-LOG-CP [7] uses

the joint statistics of gradient magnitude map and the Laplacian of Gaussian features in order to train a support vector regressor (SVR) for perceptual image quality prediction. Perception-based Image Quality Evaluator (PIQE) [8] is an opinion-unaware method and computes perceptual quality of an image through block-wise distortion estimation. First, the mean subtracted contrast normalized (MSCN) coefficients have to be determined for each pixel in the input image. Second, the input image should be divided into 16 × 16 blocks and high spatially active blocks which are identified relying on the MSCN coefficients. In each block, distortion is evaluated due to blocking artifacts and noise relying on the MSCN coefficients. A threshold criteria is also applied to classify blocks as distorted (blocking artifacts, Gaussian noise) blocks. The quality score is calculated as the mean of scores in the distorted blocks. Integrated Local NIQE (IL-NIQE)[9] is an opinion-unaware method. It integrates natural image statistics features from multiple sources such as normalized luminance, mean subtracted and contrast normalized coefficients, gradient statistics, statistics of log-Gabor filter responses and statistics of colors. Afterwards, a multivariate Gaussian model is learned from pristine image patches. Perceptual quality is quantified by measuring the deviation from the learned distribution using a Bhattacharyya-like distance. Blind MPRIs-based (BMPRI) [10] presented the concept of multiple pseudo reference images (MPRI). Specifically, the distorted images are further degraded. After, similarities between the distorted image and the MPRIs are measured. To this end, a traditional FR-IQA metric has been applied. Specifically, local binary pattern features are computed to characterize the similarities between the distorted image and the MPRIs. Finally, the similarity scores are aggregated to obtain the input image's perceptual quality. Statistical and Perceptual Features-IQA(SPF-IQA) [11] extracted different statistical (fractal dimension distribution, first digit distribution in gradient magnitude domain, then digit distribution in wavelet domain, color statistics) and perceptual features (colorfulness, global contrast factor, dark channel feature, entropy, mean of phase congruency) from the input image and fused them together. Finally, the fused feature vector is mapped onto perceptual quality scores with the help of Gaussian process regression (GPR) by applying rational quadratic kernel function. ASsessment measure with loCal descriptOR and dErivative filters (SCORER)[12] proposed a set of derivative kernels which are utilized to filter the Y, Cb, and Cr channels of the input image. As a result, a set of filtered images are obtained for further processing. Subsequently, N interest points are detected on each filtered image relying on features from accelerated segment test (FAST) [28]. Particularly, each interest point is used to describe a 3 × 3 block around the interest point by taking all values from the block. The extracted 2400-dimensional feature vectors are mapped onto perceptual quality scores with the help of a trained support vector regressor (SVR). Entropy-based IQA (ENIQA) [13] extracts features in two different domains. Namely, mutual information between color channels and the two-dimensional entropy is determined first. Subsequently, two-dimensional entropy and the mutual information of the filtered sub-band images are determined. Based on the extracted features, a support vector machine (SVM) and a support vector regressor (SVR) are trained for distortion and quality prediction, respectively. In MultiGAP (MultiGAP-SVR[14], MultiGAP-GPR [14]), an input image is run through an Inception-V3 pretrained convolutional neural network which carries out all its defined operations. Furthermore, global average pooling layers are attached to each Inception module to extract image resolution independent features. Subsequently, the features of the Inception modules are concatenated and mapped onto perceptual quality scores with the help of an support vector regressor (SVR) with Gaussian kernel function. In this study, results are obtained by Gaussain process regression (GPR) head with rational quadratic function which is also presented. Two of them BRISQUE and NIQE are implemented in MATLAB system version R2018a. A detailed description of the functions implemented in them is given in [3][4], as well as in the MATLAB reference documentation.

Both NR IQA models are based on NSS spatial domain functions [3][4]:

$$\hat{I}(i,j) = \frac{I(i,j)-\mu(i,j)}{\delta(i,j)+1} \quad (1)$$

where $i \in \{1,2 \dots M\}, j \in \{1,2 \dots N\}$ are spatial index, M and N are image dimensions, and

$$\mu(i,j) = \sqrt{\sum_{k=-K}^{K}\sum_{l=-L}^{L} \omega_{k,l}[I(i+k,j+l)-\mu(i,j)]^2} \quad (2)$$

Estimate the local mean and contrast, respectively, where $\omega = \{\omega_{k,l} | k = -K, \dots K, l = -L, \dots L\}$ is a 2D circularly-symmetric Gaussian weighting function sampled out to 3 standard deviations *(K=L=3)* and rescaled to unit volume. The

normalized brightness value of ˆI(i, j) is called MSCN (Mean Subtracted Contrast Normalized) coefficients.

The NSS functions used in the NIQE index were similarly used in the BRISQUE model. However, NIQE uses only NSS functions from a set of natural images, while BRISQUE learns features derived from both natural and distorted images, as well as human estimates of the quality of these images.

BRISQUE applies the generalized Gaussian distribution (GGD) to fit MSCN coefficients and the asymmetric generalized Gaussian distribution (AGGD) to fit pair wise products of neighboring MSCN coefficients [3].

AGGD is defined as

$$f(x;\alpha,\sigma^2)=\frac{\alpha}{2\beta\Gamma\left(\frac{1}{\alpha}\right)}\exp\left(-\left(\frac{|x|}{\beta}\right)^{\alpha}\right) \quad (3)$$

$$\text{where} \quad \beta=\sigma\sqrt{\frac{\Gamma\left(\frac{1}{\alpha}\right)}{\Gamma\left(\frac{3}{\alpha}\right)}} \quad (4)$$

The shape parameter α controls the 'shape' of the distribution while σ^2 controls the variance. AGGD is defined as:

$$f(x;v,\sigma_l^2,\sigma_r^2)=\begin{cases}\frac{v}{(\beta_l+\beta_r)\Gamma\left(\frac{1}{v}\right)}\exp\left(-\left(\frac{-x}{\beta_1}\right)^{v}\right) & x<0\\ \frac{v}{(\beta_l+\beta_r)\Gamma\left(\frac{1}{v}\right)}\exp\left(-\left(\frac{-x}{\beta_r}\right)^{v}\right) & x\geq 0\end{cases} \quad (5)$$

$$\text{where} \quad \beta_l=\sigma_l\sqrt{\frac{\Gamma\left(\frac{1}{v}\right)}{\Gamma\left(\frac{3}{v}\right)}}, \quad \beta_l=\sigma_r\sqrt{\frac{\Gamma\left(\frac{1}{v}\right)}{\Gamma\left(\frac{3}{v}\right)}} \quad (6)$$

The shape parameter v controls the 'shape' of the distribution while σ_l^2,σ_r^2 are scale parameters that control the spread on each side of the mode respectively. If $\sigma_l^2=\sigma_r^2$ then the AGGD reduces to the GGD.

In the equations (3)~(6), Γ(·) is the gamma function:

$$\Gamma(a)=\int_0^{\infty}t^{a-1}e^{-t}dt \qquad a>0 \quad (7)$$

According to the NIQE method, the quality of the distorted image is expressed as the distance between the quality aware NSS feature model and the MVG fit to the features extracted from the distorted image [4]:

$$D(v_1v_2,\sum\nolimits_1\sum\nolimits_2)=\sqrt{\left((v_1-v_2)^T\left(\frac{\sum_1+\sum_2}{2}\right)^{-1}(v_1-v_2)\right)} \quad (8)$$

Were v_1,v_2 and $\sum_1,\sum_2$ are the mean vectors and covariance matrices of the natural MVG model and distorted image's MVG (multivariate Gaussian) model.

The NIQE algorithm measures the distance between objects based on NSS (natural scene statistics) calculated from image A, and objects obtained from the image database used to train the model. Features are modeled as multivariate Gaussian distribution. The BRISQUE algorithm uses a support vector regression (SVR) model trained from given images with computed differential mean image quality (DMOS) values. The database contains images with known distortions such as compression artifacts, blurring, and noise and contains pristine versions of distorted images. The image for evaluation must have at least one of the distortions that the model has been trained on. In both cases, images are needed, which are compared in accordance with the algorithms embedded in them. Despite their common approach, BRISQUE and NIQE have a number of differences. BRISQUE requires both distorted and undistorted images and additionally requires information about the type of distortion present. The algorithm of this metric contains the mechanisms of its learning. Accordingly, if some type of distortion is absent in the image database then the efficiency of the BRISQUE algorithm is noticeably reduced. In the NIQE algorithm, instead of a set of Gaussian models corresponding to the types of distortions, only one model built on the training set is used. In this regard, this algorithm is easier and more practical to use in comparison with BRISQUE.

The purpose of this work is to perform a comparative analysis between BRISQUE and NIQE, to analyze the relationship between subjective and quantitative assessments of image quality. Research results would be useful in the area of software development for image enhancement.

2. RELATED WORK

During the research, many algorithms and objective measurement methods have been studied that can automatically predict image quality. In [15], the study compares subjective image quality assessment with three NR image quality

algorithms: BIQI, BRISQUE and NIQE for the performance of assessing images with different levels of depth of field. The results showed that a large depth of field results in a higher image quality in BRISQUE and depth of field does not affect the characteristics of the two other objective indicators and human perception. The authors of the studies [16] conduct a large-scale comparative assessment to assess the capabilities and limitations of several time-pooling strategies based on non-reference video quality assessment (VQA) of user-generated video. The study gives an insight into and general recommendations regarding the use and choice of models of temporary pools. In addition, the authors propose a model of ensemble pool that is built on the basis of high-performance models of the temporary pool. In [17], a comprehensive study of perception and analysis of the elimination of blurring was carried out using real blurred images. To quantify the performance of several modern blur removal algorithms, algorithms such as BIQI, BLIINDS2, BRISQUE, CORNIA, DIIVINE, NIQE, SSEQ are used and the correlation coefficients between subjective assessments of a person are compared. The authors of [18] prove the contradiction between distortion and the quality of perception. Distortion is measured by reference comparison metrics (FR), while visual perception measurements are measured using non-reference NR metrics: BRISQUE, NIQE and BLIINDS-II. The authors of [19] in their study propose a method for assessing image quality, called RIQMC. Further, their RIQMC methodology is compared with a large number of IQA functions, including DIIVINE, BLIINDS-II, BRISQUE, NFERM, NIQE, QAC. The same comparative experiments are carried out in the article [20]. To distinguish real biometric data from fake data, the quality measures of non-reference images (IQM) BIQI, BLIINDS-2, NIQE, DIIVINE, BRISQUE are used. As a result of the experiment compares the effectiveness of the entire IQM technique for detecting biometric counterfeiting. For some datasets, authors get a perfect separation of real and fake sample data while for other data up to 10% errors are observed. Similar studies conducted Goodall T. and Bovik A. in their work [21]. They investigate infrared images in the Long-Wavelength Infrared (LWIR) range. LWIR images are often used to detect smoke, fog and dust, especially useful in low light conditions. Using LWIR, firefighters create images of indoor heat to identify critical fire points and environmental hazards. The model proposed by the authors uses four main indicators of image quality, they are brightness, contrast, spatial resolution and heterogeneity and is coded as 4IQI. BRISQUE, NIQE, 4IQI, and a combination of all three are compared using the Receiver Operator Characteristic (ROC). Research found that BRISQUE did not show significant improvement over 4IQI, but the combination of 4IQI with BRISQUE and NIQE improved performance. A large-scale comparative analysis was carried out in [22]. Charrier C and co-authors are conducting a comparative study of seven known image quality algorithms: BIQI, DIIVINE, BLIINDS, BLIINDS-II, BIQA, BRISQUE, and NIQE. The experiments are performed on three publicly available image databases: LIVE, TID2008, and CSIQ. The results of measuring and comparing the effectiveness of the algorithms are carried out using the Spearman correlation coefficient. In [23], a study of evaluating images with a 360-degree view is presented. It compares the effectiveness of objective image quality assessment (IQA) methods in assessing the quality of compressed 360-degree images. First, a database of compressed 360-degree images is created using the CVIQD2018 image database. Then compares 16 indicators of comparison full reference and 5 functions of comparison no reference, such as BRISQUE, NIQE, GMLF, QAC, SISBLIM. Finally, the correlation between the indicated measures and subjective assessments is calculated. As a result of the experiment, the authors concluded that structural information, visibility and geometric distortion compensation are critical to assess the quality of compressed 360-degree images. The main goal of [24] paper is to perform a comparative study of seven well known no-reference image quality algorithms. To test the performance of these algorithms, three public databases are used. The Spearman rank ordered correlation coefficient is utilized to measure and compare the performance. In addition, an hypothesis test is conducted to evaluate the statistical significance of performance of each tested algorithm. In [25] paper, a new preprocessing algorithm to qualify images of different pollen grains for further processing is proposed. This algorithm provides a score related to the sharpness of the image and will be used to automatically adjust the focal length of a microscope that magnifies the image. The obtained score has been compared to four quality metrics generally used to estimate the clarity of an image and to a reference made by a human. The results of the simulations show that the proposed algorithm combines better performance with low complexity on the set of images. In [26] study authors compares four state-of-the-art NR metrics NIQE,

BIQES, NIQE-K and BRISQUE. In order to evaluate these algorithms, they study four No-Reference (NR) quality assessment metrics in terms of correlation with perceived scores of experts. These scores were obtained through subjective tests conducted on ultrasound (US) livers images. Results show that metric NIQE performs the best for assessing the quality of US images. However, further study is needed for the development of more suitable NR metrics.

3. INITIAL DATA FOR EXPERIMENTS

The study used the MATLAB software package as a tool. The experimental data were images with artificially created distortions and with expert assessments of their quality from the public databases TID2013 [27], CISQ [28] and LIVE [29].

The TID2013 Image Database contains 25 reference images. All images have 24 types of distortions applied. Each type of distortion is represented by five variants of images. In total, the database contains 3000 distorted color images. Additionally, for each distorted image, subjective MOS scores were obtained, obtained by human experts when comparing the distorted images with the reference in the scale [0, 9].

The CISQ image database contains 866 quality images. 30 reference images are distorted by JPEG compression, JP2K compression, Gaussian blur, Gaussian white noise, Gaussian pink noise or contrast change. To assess the quality, the experts were asked to arrange the distorted images horizontally on the monitor in accordance with their visual quality. After equalization and normalization, the resulting DMOS values are written in the range [0, 1], where a lower value indicates better subjective image quality.

They have been distorted using the following types of distortion: JPEG2000 and JPEG compression, RGB white noise, Gaussian blur, and bit errors in the JPEG2000 bitstream when transmitted over a simulated fast fading Rayleigh channel. MOS values are in the range [0, 100], higher values indicate better quality.

4. PLAN OF THE EXPERIMENT

In most cases, distortions such as noise, blur, contrast and compression affect image quality. In this case, in our research, four types of distortions were selected: adding additive Gaussian noise to the original image, Gaussian blur, changing the contrast, and JPEG2000 compression (Fig. 1).

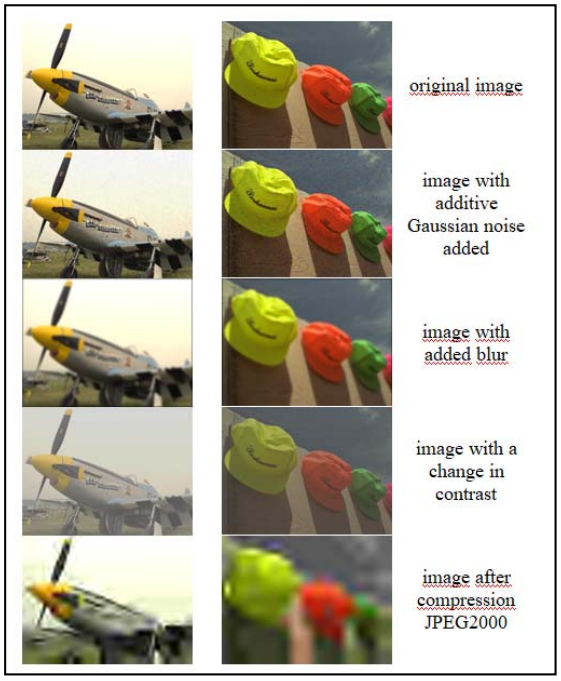

Figure1: Examples of images from the TID2013 database

Image quality estimates are calculated using the NIQE, BRISQUE functions and the averaged NIQE + BRISQUE method. Estimates with the averaged NIQE + BRISQUE method were obtained as the arithmetic mean of the values of the normalized NIQE and BRISQUE functions.

BRISQUE and NIQE grading scales are different. For example, the ratings of the same image are BRISQUE = 72.7539 and NIQE = 1.8. To compare the results between the objective and visually evaluated estimates we normalized estimates using equation (9) that all estimates are in the range [0, 1].

$$x' = \frac{X - X_{MIN}}{X_{MAX} - X_{MIN}} \qquad (9)$$

In the equation, the variables X and x' are the original image quality score and the normalized score. X_{MIN} and X_{MAX} are the lowest and highest scores.

By definition of NIQE and BRISQUE the lower the value the better the picture. MOS estimates in the databases TID2013 and LIVE, on the contrary, the more the better the image. For ease of comparison, MOS estimates normalized by the formula (10)

$$x' = 1 - \frac{X - X_{MIN}}{X_{MAX} - X_{MIN}} \qquad (10)$$

Further, the correlation of Pearson, Kendall and Spearman [30] are analyzed between visual assessments of experts and quantitative assessments of image quality, as well as between the values of two compared measures.

5. DISCUSSION OF THE EXPERIMENTAL RESULTS

All the interference introduced into a digital image is commonly called noise. Noise degrades its quality and makes it difficult for humans to visualize images. Therefore, evaluating noisy images is an important task in image analysis. In our experiment, 125 images from the TID2013 database, 150 images from the CSIQ database and 174 images from the LIVE database are selected to assess the quality of digital images distorted by additive noise. They were obtained quantitative estimates of the quality of each test image. Image evaluation for NIQE varied in TID2013 from 3.97 to 14.92, in CSIQ from 3.12 to 16.39, in LIVE from 2.21 to 70.23. The lowest BRISQUE score was 15.22 in TID2013, 5.74 in CSIQ, and 2.35 in LIVE and the highest was 45.64, 46.30 and 71.83, respectively, on TID2013, CSIQ and LIVE image databases. The results are recorded in Table 1.

Table 1: Range of estimates for tested images Gaussian noise

	Image bases		
	TID2013	CSIQ	LIVE
Number of images	125	150	174
$NIQE_{MIN}$	3.96	3.12	2.21
$NIQE_{MAX}$	14.92	16.39	70.23
$BRISQUE_{MIN}$	15.22	5.74	2.35
$BRISQUE_{MAX}$	45.64	46.30	71.83
MOS_{MIN}	3.4	0	0
MOS_{MAX}	5.9	0.5	1.9

We compared the quality metrics of each image with two functions. To select more effective of these was calculated the Pearson correlation, Spearman and Kendall. The correlation coefficients are shown in Table 2.

Assess the quality of images obtained by NIQE function correlated with the estimates obtained function BRISQUE. Pearson's correlation coefficient is higher than 0.73 for all images. The BRISQUE and NIQE functions give positively correlated estimates of image quality with Kendall's coefficients in the range [0.56, 0.87]. Spearman correlation coefficient between the functions and BRISQUE NIQE is above 0.77. Table 2 shows a good correlation between the MOS and quantitative estimates BRISQUE, NIQE and NIQE + BRISQUE. For the images used in the current experiment, all image quality assessments obtained using three objective indicators correlate well with the visual assessments of experts. NIQE function values for images from the database LIVE show a high correlation with MOS values. The correlation coefficients of Pearson, Kendall, and Spearman are 0.95, 0.88, 0.98, respectively. BRISQUE performance is correlated with MOS performance. For them, the correlation coefficients of Pearson, Kendall and Spearman vary in the range [0.65, 0.99]. The correlation coefficients obtained between the averaged method NIQE + BRISQUE and MOS also give high values: Pearson coefficient is above 0.86, Kendall coefficient is above 0.67 and Spearman coefficient is above 0.87.

Table 2: Correlation coefficients between quantitative and visual assessments of image quality for distortions of additive Gaussian noise

		NIQE	BRISQUE	NIQE + BRISQUE
Image Database TID2013				
Pearson	**NIQE**		0.80	
	BRISQUE	0.80		
	MOS	0.80	0.86	0.88
Kendall	**NIQE**		0.66	
	BRISQUE	0.66		
	MOS	0.63	0.70	0.70
Spearman	**NIQE**		0.85	
	BRISQUE	0.85		
	MOS	0.83	0.83	0.89
Image Database CSIQ				
Pearson	**NIQE**		0.73	
	BRISQUE	0.73		
	MOS	0.79	0.82	0.86
Kendall	**NIQE**		0.56	
	BRISQUE	0.56		
	MOS	0.64	0.65	0.67
Spearman	**NIQE**		0.77	
	BRISQUE	0.77		
	MOS	0.84	0.83	0.87

Image Database LIVE				
Pearson	NIQE		0.79	
	BRISQUE	0.79		
	MOS	0.95	0.71	0.87
Kendall	NIQE		0.87	
	BRISQUE	0.87		
	MOS	0.88	0.93	0.92
Spearman	NIQE		0.98	
	BRISQUE	0.98		
	MOS	0.98	0.99	0.99

At the next stage of the research, the results of the experimental determination of the image quality assessment are considered under the assumption that the ideal image was Gaussian blurred. An array of estimates for each image using the BRISQUE, NIQE and NIQE + BRISQUE functions are received. Also a range of estimates for each investigated measure and for MOS (table 3) are identified.

Table 3:Range of estimates for tested images Gaussian blur

	Image bases		
	TID2013	CSIQ	LIVE
Number of images	125	150	174
$NIQE_{MIN}$	2.11	2.57	2.21
$NIQE_{MAX}$	7.29	8.39	7.17
$BRISQUE_{MIN}$	3.82	2.22	2.35
$BRISQUE_{MAX}$	63.59	74.03	80.46
MOS_{MIN}	1.25	0.01	0
MOS_{MAX}	6.34	0.99	15

Further, the correlations of Pearson, Kendall and Spearman are calculated between the visual assessments of experts and different quantitative assessments of the image quality. Table4 represents the results of the relationship between visual and quantitative assessments of image quality. Analyzing Table 3, it can be seen that all measures are positively correlated with MOS scores. NIQE function correlates with MOS having a Pearson coefficient values above 0.70, Kendall coefficient above 0.56 and Spearman coefficient above 0.78. BRISQUE scores correlate with MOS scores with Pearson, Kendall and Spearman scores 0.83 (TID2013), 0.90 (CSIQ) and 0.98 (LIVE) respectively.

Table 4: Coefficients of correlation between quantitative and visual assessments of image quality for distortions Gaussian blur

		NIQE	BRISQUE	NIQE + BRISQUE
Image Database TID2013				
Pearson	NIQE		0.81	
	BRISQUE	0.81		
	MOS	0.83	0.83	0,87
Kendall	NIQE		0.65	
	BRISQUE	0.65		
	MOS	0.64	0.65	0,69
Spearman	NIQE		0.84	
	BRISQUE	0.84		
	MOS	0.82	0.84	0,87
Image Database CSIQ				
Pearson	NIQE	0.82	0,82	
	BRISQUE	0.88		
	MOS		0,75	0,86
Kendall	NIQE	0.63	0,63	
	BRISQUE	0.68		
	MOS		0,56	0,65
Spearman	NIQE	0.84	0,84	
	BRISQUE	0.88		
	MOS		0,78	0,86
Image Database LIVE				
Pearson	NIQE		0,89	
	BRISQUE	0.89		
	MOS	0.70	0,74	0,74
Kendall	NIQE		0,73	
	BRISQUE	0.73		
	MOS	0.73	0,90	0,85
Spearman	NIQE		0,91	
	BRISQUE	0.91		
	MOS	0.91	0,98	0,96

The correlation coefficients obtained between NIQE + BRISQUE and MOS also give a positive value in all measures of correlation. Pearson coefficient value equal to 0.87 (TID2013), Kendall - 0.90 (LIVE) and Spearman - 0.98 (LIVE). The indicators obtained by the BRISQUE function correlate with the NIQE function showing a Pearson coefficient of 0.81 or higher. BRISQUE and NIQE provide positively correlated estimates of image quality with Kendall coefficients above

0.63. Spearman correlation coefficient between the functions BRISQUE and NIQE is above 0.84.

The correctness of the image quality assessment depends not only on the used measure but also on the type of image distortion. One of the indicators of image quality is its contrast. Visually, the contrast of an image is perceived as the difference between light and dark areas of the image [1].

Similar actions are carried out in an experiment with images from the TID2013 and CSIQ databases with distorted contrast (Table 5). The LIVE database is not used as it does not contain images with altered contrast. After obtaining estimates, they are normalized according to the formula (1) and their correlation coefficients are calculated between parameters and values MOS investigated quality assessment functions. The results are recorded in Table 6.

Table 5: Range of estimates for the tested images with distorted contrast

	Image bases	
	TID2013	CSIQ
Number of images	125	116
$NIQE_{MIN}$	1.98	2.27
$NIQE_{MAX}$	8.12	8.53
$BRISQUE_{MIN}$	2.41	2.85
$BRISQUE_{MAX}$	43.87	53.68
MOS_{MIN}	0.58	0.01
MOS_{MAX}	7.21	0.68

Table 6. Coefficients of correlations between quantitative and visual assessments of image quality with distorted contrast

		NIQE	BRISQUE	NIQE + BRISQUE
Image Database TID2013				
Pearson	**NIQE**		0.58	
	BRISQUE	0.58		
	MOS	0.06	0.07	0.19
Kendall	**NIQE**		0.25	
	BRISQUE	0.25		
	MOS	0.11	0.06	0.13
Spearman	**NIQE**		0.36	
	BRISQUE	0.36		
	MOS	0.16	0.09	0.18
Image Database CSIQ				
Pearson	**NIQE**		0.45	
	BRISQUE	0.45		
	MOS	0.08	0.19	0.19
Kendall	**NIQE**		0.22	
	BRISQUE	0.22		
	MOS	0.00	0.14	0.13
Spearman	**NIQE**		0.32	
	BRISQUE	0.32		
	MOS	0.00	0.20	0.18

An interesting feature manifested itself when evaluating the quality of images with altered contrast. All correlation coefficients show low results for the studied measures. Thus, it has been shown experimentally that quantitative assessments correlate poorly with visual assessments.

Evaluation of the image restoration quality deserves special attention. Since the images contain information that is redundant with the entry in the file of the memory is wasted for storing redundant data. Important applications include camera calibration, robot navigation and machine vision, image matching, and pattern recognition. We obtained scalable masks for detecting angles in images [31,32,33]. Compression algorithms reduce the amount of redundant information. The algorithm used in the JPEG2000 standard is based on the wavelet decomposition of an image [34]. At this stage of the experiment, the estimates of the image quality with JPEG2000 compression are calculated and the ranges of estimates for their normalization are determined (Table 7).

Table 7: Ranges of estimates for tested images with JPEG2000 compression

	Image bases		
	TID2013	CSIQ	LIVE
Number of images	125	150	227
$NIQE_{MIN}$	3.32	2.35	2.05
$NIQE_{MAX}$	9.15	9.15	9.23
$BRISQUE_{MIN}$	6.96	4.50	2.34
$BRISQUE_{MAX}$	73.83	73.30	70.86
MOS_{MIN}	0.65	0	0
MOS_{MAX}	6.12	3.15	3.15

A correlation study is performed, calculated quantitative scores with visual assessments of the quality of the tested images. The estimates obtained using the presented indicators

for the TID2013, CSIQ and LIVE image database are generally in good agreement with the results of visual examination. The correlation coefficients between NIQE and BRISQUE are presented in the range [0.77, 0.93] (Table 8).

Table 8. Coefficients of correlations between quantitative and visual assessments of image quality with JPEG2000 compression

		NIQE	BRISQUE	NIQE + BRISQUE
Image Database TID2013				
Pearson	**NIQE**		0.73	
	BRISQUE	0.73		
	MOS	0.67	0.80	0.79
Kendall	**NIQE**		0.57	
	BRISQUE	0.57		
	MOS	0.53	0.66	0.62
Spearman	**NIQE**		0.76	
	BRISQUE	0.76		
	MOS	0.74	0.86	0.83
Image Database CSIQ				
Pearson	**NIQE**		0.86	
	BRISQUE	0.86		
	MOS	0.88	0.82	0.88
Kendall	**NIQE**		0.68	
	BRISQUE	0.68		
	MOS	0.69	0.63	0.69
Spearman	**NIQE**		0.87	
	BRISQUE	0.87		
	MOS	0.87	0.83	0.88
Image Database LIVE				
Pearson	**NIQE**		0.86	
	BRISQUE	0.86		
	MOS	0.86	0.83	0.87
Kendall	**NIQE**		0.69	
	BRISQUE	0.69		
	MOS	0.79	0.77	0.78
Spearman	**NIQE**		0.89	
	BRISQUE	0.89		
	MOS	0.93	0.91	0.89

To calculate quantitative estimates, the functions implemented in the MATLAB system are used: ***niqe*** and ***brisque***. Table 9 contains averaged values of the computation time of these functions. It can be seen that in all cases the ***niqe*** function is faster than ***brisque***.

*Table 9. Measurement of the execution time of the **niqe** and **brisque** functions*

Distortion type	Image quantity	Expanding images	Speed of the running program (s)	
			niqe	brisque
TID2013				
noise	125	512*384	6.97	9.36
blur	125	512*384	7.93	8.29
contrast	125	512*384	6.16	6.36
compression	125	512*384	7.13	10.46
CSIQ				
noise	150	512*512	28.29	30.87
blur	150	512*512	28.23	28.34
contrast	116	512*512	8.97	8.59
compression	150	512*512	9.48	11.10
LIVE				
White Noise	174	768*512 480*720 627*482	14.37	15.03
Gaussian Blur	174	768*512 480*720 632*505	15.84	17.33
JPEG2000	227	768*512 480*720 627*482	22.08	23.79

CONCLUSION

Experiments to assess the quality of images have shown that NIQE, BRISQUE and NIQE + BRISQUE methods can be applied to TID2013, CSIQ and LIVE images with artificially created distortions such as additive Gaussian noise, Gaussian blur and loss in the compression process with the JPEG2000 algorithm. All quality measures have shown good results. Their correlation with expert estimates is more than 0.7.

The NIQE, BRISQUE, and NIQE + BRISQUE measures should not be used to assess the quality of images with distorted contrast as they have low correlation with subjective assessments of image quality.

BRISQUE measure shows the best results in the evaluation of image quality with such distortions as the additive Gaussian noise.

Measure NIQE showed high correlation between quantitative and visual scores for Gaussian blurred images.

For more accurate assessment is recommended to use the arithmetic mean of the values of the two functions NIQE and BRISQUE.

This study shows that the average score performs well when evaluating images with distortions such as additive Gaussian noise, Gaussian blur, and JPEG2000 compression.

The presented research results investigate only small class of possible image distortions. We will extend the studied types of image distortions.

The investigated IQA metrics can be used to quantitatively assess the quality of images with distortions of the indicated classes. For other types of distortion, additional research is required.

In the future, we plan to investigate machine learning-based image quality assessment metrics.

REFRENCES:

[1] Moorthy, Anush Krishna, and Alan Conrad Bovik, "Blind image quality assessment: From natural scene statistics to perceptual quality", *IEEE transactions on Image Processing,* Vol. 20, No.12, 2011, pp. 3350-3364.

[2] Saad, Michele A., Alan C. Bovik, and Christophe Charrier, "Blind image quality assessment: A natural scene statistics approach in the DCT domain", *IEEE transactions on Image Processing,* Vol. 21, No.8, 2012, pp. 3339-3352.

[3] Mittal, Anish, Anush Krishna Moorthy, and Alan Conrad Bovik, "No-reference image quality assessment in the spatial domain", *IEEE Transactions on image processing*, Vol.21, No.12, 2012, pp. 4695-4708.

[4] Mittal, Anish, Rajiv Soundararajan, and Alan C. Bovik, "Making a “completely blind” image quality analyzer", *IEEE Signal processing letters*, Vol.20, No.3, 2012, pp.209-212.

[5] Liu, Lixiong, et al. "No-reference image quality assessment in curvelet domain", *Signal Processing: Image Communication,* Vol. 29, No.4, 2014, pp. 494-505.

[6] Liu, Lixiong, et al, "No-reference image quality assessment based on spatial and spectral entropies", *Signal Processing: Image Communication,* Vol. 29, No.8, 2014, pp. 856-863.

[7] Xue, Wufeng, et al, "Blind image quality assessment using joint statistics of gradient magnitude and Laplacian features", *IEEE Transactions on Image Processing,* Vol. 23, No.11, 2014, pp. 4850-4862.

[8] Venkatanath, N., et al, "Blind image quality evaluation using perception based features", *2015 Twenty First National Conference on Communications (NCC)*, IEEE, 2015, pp.1-6

[9] Zhang, Lin, Lei Zhang, and Alan C. Bovik, "A feature-enriched completely blind image quality evaluator", *IEEE Transactions on Image Processing,* Vol. 24, No. 8, 2015, pp. 2579-2591.

[10] Min, Xiongkuo, et al, "Blind image quality estimation via distortion aggravation", *IEEE Transactions on Broadcasting* , Vol. 64, No. 2, 2018, pp. 508-517.

[11] Varga, Domonkos, "No-reference image quality assessment based on the fusion of statistical and perceptual features", *Journal of Imaging,* Vol. 6, No. 8, 2020, pp.75.

[12] Oszust, Mariusz, "Local feature descriptor and derivative filters for blind image quality assessment", *IEEE Signal Processing Letters,* Vol. 26, No.2, 2019, pp. 322-326.

[13] Chen, Xiaoqiao, et al, "No-reference color image quality assessment: from entropy to perceptual quality", *EURASIP Journal on Image and Video Processing,* Vol. 2019, No. 1, 2019. pp. 1-14.

[14] Varga, Domonkos, "Multi-pooled inception features for no-reference image quality assessment", *Applied Sciences,* Vol. 10, No. 6, 2020, p. 2186.

[15] Zhang, Tingting, et al, "Depth-of-field effect in subjective and objective evaluation of image quality", *Proceedings of the 2018 Conference on Research in Adaptive and Convergent Systems*, 2018, pp. 308-312.

[16] Tu, Zhengzhong, et al, "A comparative evaluation of temporal pooling methods for blind video quality assessment", *2020 IEEE International Conference on Image Processing (ICIP)*, IEEE, 2020, pp. 141-145

[17] Lai, Wei-Sheng, et al, "A comparative study for single image blind deblurring", *Proceedings of the IEEE Conference on Computer Vision and Pattern Recognition*, 2016, pp. 1701-1709.

[18] Blau, Yochai, and Tomer Michaeli, "The perception-distortion tradeoff", *Proceedings of the IEEE Conference on Computer Vision and Pattern Recognition*, 2018, pp. 6228-6237.

[19] Gu, Ke, et al, "The analysis of image contrast: From quality assessment to automatic enhancement", *IEEE transactions on cybernetics,* Vol. 46, No. 1, 2015, pp. 284-297.

[20] Söllinger, Dominik, Pauline Trung, and Andreas Uhl, "Non-reference image quality assessment and natural scene statistics to counter biometric sensor spoofing", *IET Biometrics,* Vol. 7, No. 4, 2018, pp. 314-324.

[21] Goodall, Todd, and Alan C. Bovik, "No-reference task performance prediction on distorted LWIR images", *2014 Southwest*

Symposium on Image Analysis and Interpretation, IEEE, 2014, pp. 89-92.

[22] Charrier, Christophe, Abdelhakim Saadane, and Christine Fernandez-Maloigne, "Comparison of no-reference image quality assessment machine learning-based algorithms on compressed images", *Image Quality and System Performance XII*, Vol. 9396, International Society for Optics and Photonics, 2015, p. 939610.

[23] Sun, Wei, et al, "A large-scale compressed 360-degree spherical image database: From subjective quality evaluation to objective model comparison", *2018 IEEE 20th international workshop on multimedia signal processing (MMSP)*, IEEE, 2018, pp. 1-6.

[24] Nouri, Anass, et al, "Statistical comparison of no-reference images quality assessment algorithms", *2013 Colour and Visual Computing Symposium (CVCS)*, IEEE, 2013, pp. 1-5.

[25] Kadaikar, Aysha, et al, "Sharp Images Detection for Microscope Pollen Slides Observation", *Asian Conference on Intelligent Information and Database Systems*, Springer, Cham, 2019, pp. 661-671.

[26] Outtas, Meriem, et al, "Evaluation of No-reference quality metrics for Ultrasound liver images", *2018 Tenth International Conference on Quality of Multimedia Experience (QoMEX)*, IEEE, 2018, pp. 1-3.

[27 Ponomarenko, Nikolay, et al, "Image database TID2013: Peculiarities, results and perspectives", *Signal processing: Image communication*, Vol. 30, 2015, pp. 57-77.

[28] Larson, Eric Cooper, and Damon Michael Chandler, "Most apparent distortion: full-reference image quality assessment and the role of strategy", *Journal of electronic imaging,* Vol. 19, No. 1, 2010, p. 011006.

[29] Sheikh, Hamid R., Muhammad F. Sabir, and Alan C. Bovik, "A statistical evaluation of recent full reference image quality assessment algorithms", *IEEE Transactions on image processing,* Vol. 15, No. 11, 2006, pp. 3440-3451.

[30] Starovoytov V.V., Eldarova E.E., Iskakov K.T., "Comparative analysis of the SSIM index and the pearson coefficient as a criterion for image similarity", *Eurasian Journal of Mathematical and Computer Applications,* Vol. 8, No. 1, 2020, pp. 76-90. DOI: 10.32523/2306-6172-2020-8-1-76-90

[31] I. G. Kazantsev, B. O. Mukhametzhanova, and K. T. Iskakov, "Detection of the corner structures in 3D arrays using scalable masks" *Siberian Electronic Mathematical Reports*, Vol. 18, 2021, pp. 61–71. DOI 10.33048/semi.2021.18.006

[32] I. G. Kazantsev, B. O. Mukhametzhanova, K. T. Iskakov, and T. Mirgalikyzy, "Detection of the Corner Structures in Images by Scalable Masks", *Journal of Applied and Industrial Mathematics*, Vol. 14, 2020, pp. 73–84. DOI 10.33048/SIBJIM.2020.23.107

[33] Orazbayev, B., Assanova, B., Bakiyev, M., Krawczyk, J., Orazbayeva, K., "Methods of model synthesis and multi-criteria optimization of chemical-engineering systems in the fuzzy environment", *Journal of Theoretical and Applied Information Technology*, Vol. 98, No. 6, 2020, pp. 1021–1036.

[34] Sun, Wen, Fei Zhou, and Qingmin Liao, "MDID: A multiply distorted image database for image quality assessment", *Pattern Recognition,* Vol. 61, 2017, pp. 153-168.